Lab report

Suzuki Reaction: Investigating Reactivity and Functional Group Effects through Aryl Halide and Boronic Acid Variation, Esterification, and Amidation

Shahan Khan, Kaysa Sekhavati, Ceri House, Georgia Reynolds, Sofia Thalassitis

Abstract: The Suzuki cross coupling (SCC) reaction remains to be one of the most widely used and important reactions to form C - C bonds. This is primarily due its remarkable functional group tolerance and its ability to tolerate sterically hindered molecules. Our initial focus centred on altering halide position and type while maintaining other parameters constant. Revealing the highest reactivity occurring when iodide was positioned at the para position. Subsequently, we explored the effects of varying the boronic acid through modification of attached substituents with variable electron releasing potential. The study next transitioned to exploring the influence of electron withdrawing and donating groups (EWG/EDG) on the efficiency of esterification, while additionally conducting amidation reactions on the SCC products. EDGs on the boronic acid were found to increase the rate of SCC reactions while EWG were found to increase the rate of esterification. Amidation of SCC 1 products yielded inconclusive results due to low yield and impurities present in the starting material. Our study underscores the significance of these findings in advancing the design of optimised SCC reactions. These insights hold promise in the development of tailored approaches to synthesising precise molecules which in turn have the potential for substantial implications in a diverse array of chemical industries.

Introduction

The Suzuki cross coupling reaction is a powerful organic synthetic route owing to its versatility and relative ease in achieving the formation of new C – C bonds, which are extremely important for synthesis.[1] First introduced in 1979 by Akira Suzuki and co-workers who were awarded the 2010 noble prize for this work SCC reactions have been a staple in various industries ranging from pharmaceuticals, polymers, fine chemicals, and materials.[2],[3] The formation of these new C – C bonds is achieved via the utilisation of an organoboronic acid or ester coupling with an organohalide using a palladium complex catalyst alongside a base. [3]

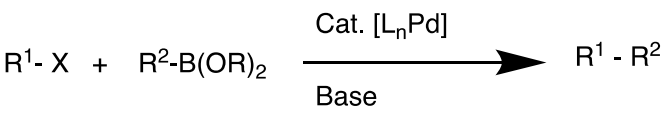

Figure 1. General reaction scheme of a Suzuki cross coupling reaction
X = Halide

This study was prompted by the remarkable surge in both utilization and research interest witnessed in recent years.[4] This is due to its incredible functional group tolerance as well as its capability for accommodating sterically hindered molecules. [5],[6]

This cross-coupling reaction consists of a catalytic cycle consisting of 3 major steps: Oxidative addition, transmetalation and reductive elimination, a general schematic of the catalytic cycle can be seen in Figure 2.[7]

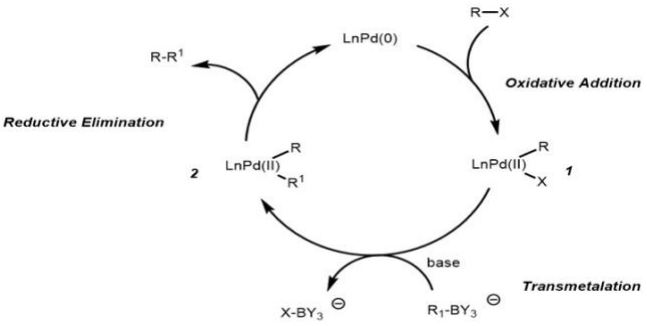

Figure 2. General mechanism of Suzuki coupling

Herein, we seek to explore the influence of positional isomerism and halide variation in SCC reactions, while also examining the effects of varying boronic acids. Additionally, we aim to assess the efficiency of esterification and amidation reactions on the resulting products. Aryl halides (ArX, where X = Br, I) underwent reactions with X positioned at the ortho, meta, and para positions, aligning with previous work carried out by Hoffmann et al. where the impact of halide position and nature were investigated.[8] Experiment 2 consisted of 4-iodobenzoic acid coupled with an aryl boronic acid, substituting the para position with varying EWG and EDGs. Further esterification and amidation experiments were conducted on SCC products, in order to study the influence of EWG and EDGs on reaction rates. These findings are crucial as it paves the way to more efficient design of SCC

reactions for the formation of C – C bonds. Such advancements are fundamental in the context of synthesis of functionalised molecules with precise electronic properties allowing contributions to various fields in chemistry.

Results and discussion

Suzuki cross coupling 1

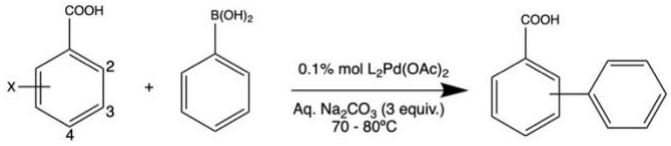

Figure 3. General reaction scheme of Suzuki coupling reaction 1.

We investigated how the position and identity of the halide in the aryl halide would affect the Suzuki cross coupling reaction using phenylboronic acid and different halo-substituted benzoic acids (figure 3). Factors that remained constant throughout this experiment included: the Boronic acid, mol % of catalyst, the base, and the catalyst. This approach ensured that the investigation solely focused on assessing the impact of the nature and position of the halide on the reaction rate.

Halide	Position of X	Time taken (mins)	Yield (%)
I	2	>24	48
Br	2	90	13
Br	3	90	57
Br	4	70	70
I	4	45	64

Table 1. Data collected from reaction 1.
Shaded = unsuccessful, unintended product formed

Table 1 provides a comparison of reaction rates for different halide positions and types. From the data it can be deduced that position 4 is the most reactive as it led to the highest yield as well as the lowest reaction time. This follows the trend observed by Hoffmann et al. where the reaction rate increased strongly for the para position.[8] They also reported an increased reaction rate when the halide was exchanged from a bromide to an iodide. This discrepancy in reaction rates can be understood by considering rate of the oxidative addition, where the R – X bond is broken. Hence, if the bond strength of R - X is weaker it will result in a faster reaction. The C – I bond has a bond dissociation energy (BDE) of 209 kJ/mol whereas a C – Br bond has a BDE of 280 kJ/mol.[9] The lower BDE of the C–I bond signifies its weakened strength, leading to an accelerated oxidative addition step. An additional perspective can be gained by considering the kinetics involved. Cleaving the C – Br bond as compared to C – I is a more endothermic process due to the higher BDE, consequently the transition state will appear later according to the Hammond postulate and ergo a higher activation energy [10]. This decrease in BDE primarily arises from the larger orbital size of iodine, which results in weaker overlap with the carbon of the ring. This difference in orbitals size can more clearly be seen through the atomic radius of both halides; while iodine holds an atomic radius of 1.40 Å, bromine possesses a smaller radius with 1.15 Å.[11]

Additionally, the enhanced reactivity of the para position is likely due to the lack of steric hindrance imposed by the carboxylic acid that is present in the other positions, this is especially prevalent in the ortho position. This can be appreciated with iodine at position 2 which required 24 hours to proceed and yielded an incorrect product. This is evident from the ^{13}CNMR analysis, which revealed the absence of the expected 11 and presence of 7 peaks, (synthesis of 2-biphenylbenzoic acid **(1a)**). Likewise, the yield of the product with bromine at position 2 was significantly lower.

The results of this experiment highlight the need for careful consideration of the position and character of the aryl halide as they effect the rate of the oxidative.

Suzuki cross coupling 2

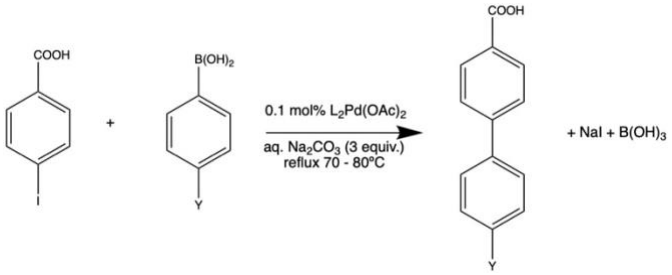

Figure 4. General reaction mechanism of Suzuki coupling reaction 2.

Our second experiment consisted of the same reaction as SCC 1 however the aryl halide was kept constant and the boronic acid was varied. For this reaction 4 – iodobenzoic acid was chosen as the aryl halide of choice due to the C – I bond being the most readily cleaved.

R group	Time take (min)	Yield (%)	EWG or EDG
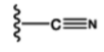	90	20	EWG
	90	24	EWG
F	90	52	EWG & EDG
Cl	60	63	EWG & EDG
Me	30	66	EDG
OMe	30	41	EDG

Table 2. Data collected from Suzuki 2

The parameters measured were time taken, yield percentage, and the type of electron releasing group associated with differing Y groups in our experiment (table 2). The methoxy group was reported to take 30 minutes whereas the cyano group was identified to take

150 minutes. From table 2 we can discern a trend where the rate of reaction increases as the electronegativity of the substituent decreases. This can be explained by the fact that increasing the electron-donating ability of the para-substituent increases the nucleophilicity of the boronic acid, making it more reactive toward SCC reactions. [12] This is achieved by increasing the bond polarity of the C – B bond and thus making it weaker and easier to overcome in the transmetalation step.

One problem with using arylboronic species is the decomposition and side reactions of the arylboronic acids. This is prevalent in all SCC reactions and is especially prevalent with the use of a boronic ester. Protodeboronation is one of the pathways that this decomposition can occur [13]. This is when the boronic acid undergoes a base catalysed reaction with water to release an arene and the boronic acid (figure 5). [13]

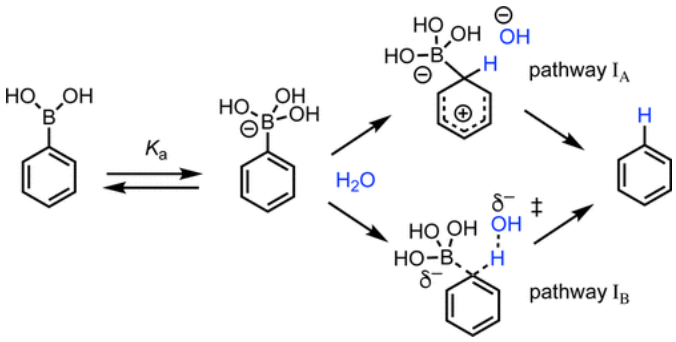

Figure 5. Protodebornation mechanism

The driving force for this acid-base reaction is the protonation of the arene and the release of the boronic acid. During the synthesis of 4-(4-acetylphenyl) benzoic Acid **(1b)** it was found that upon recrystallisation and hot filtration a white powder of inorganic material was left behind that had failed to dissolve in isopropanol. This is likely the product of protodeboronation and is likely the compound acetophenone. Although, it must be noted that further tests were not performed to confirm the identity of this compound. Protodeboronation side reactions can be averted in future experiments through consideration of using alternative boronates, such as tetrahedral boronates.[18] These have been proven to be effective in inhibiting the undesired side reactions by saturation of the normally vacant p-orbital of the boron. The most effective boronate in preventing the decomposition pathway are RBF_3K and RB[MIDA] as demonstrated by St. Denis et al in their research in to optimising conditions of SCC reactions.[18]

Esterification

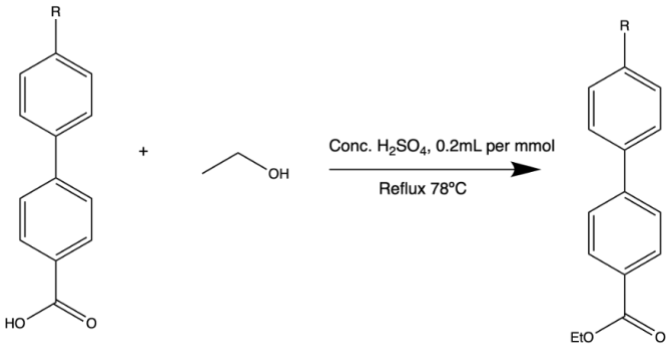

Figure 6. General reaction scheme of esterification
R group from boronic acid of SCC 2

Products from SCC 2 were used to explore the influence of these differing substituents in an esterification reaction. Here we kept all parameters constant such as the nucleophile ethanol, Conc. 18 M H_2SO_4 and kept the reaction under reflux at 78ºC. These parameters kept constant ensured we were able to solely investigate the effect of the substituent on the reaction. The resulting impacts on the reaction can be seen in Table 3.

R group	Time taken (min)	Yield (%)	EWG or EDG
F	150	32	EW - induction
	240	22	EW
Cl	300	18	ED
Me	300	21	ED
OMe (unsuccessful)	>24 hours	76	ED

Table 3. Data collected from esterification.
EWG/EDG = Electron withdrawing/donating group

The choice of ethanol over methanol was based on its larger size, resulting in lower volatility. This characteristic allowed for better control over its reactivity over the course of the reaction. [14,17] From the data analysis we can infer that EWG's facilitates the esterification as is evident by the decreasing reaction time when electron withdrawing ability increases. EWG's have the ability to draw electron density away from the carbon of the carbonyl group, rendering it more electrophilic.[16] As a result, nucleophilic ethanol exhibits faster reactivity in the presence of such groups. Conversely EDG's elucidate the reverse effect, they push electron density towards the carbonyl which decreases its electrophilicity and thus decreases the reaction time. [16] This results from the breakage of the C – O having the highest energy barrier with $\Delta G^{\ddagger}$ = 20.0 kcal mol^{-1} and thus it is the rate determining step and consequently any changes to the electrophilicity of the carbonyl willhave the larg est effect on the reaction time. [15]

These effects induced by these EWG/EDG's are largely associated with resonance.

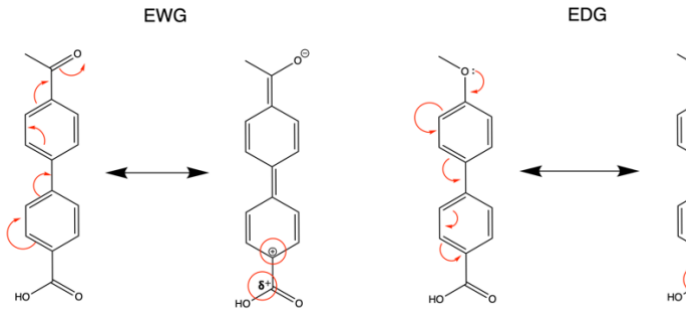

Figure 6. Resonance forms of EDG and EWG

In the resonance form of the EWG case we can see we have a positive charge next to the carbonyl (figure 7). This suggests less electron density near the electrophile, making it more electrophilic. Conversely the negative charge adjacent to the electrophile for the EDG case indicates heightened electron density surrounding the carbonyl. This postulates the increased reaction rate for the EW substituents due to the increasing reactivity of the carbonyl carbon.

Amidation

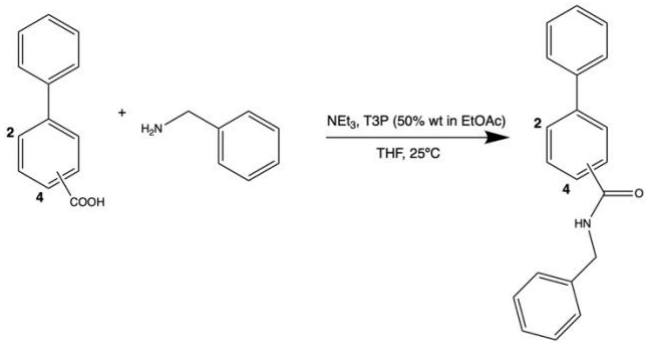

Figure 7. Note: Resulting carboxylate can be an acetic acid

Following esterification, we conducted further experiments to explore the reactivity of these SCC products. On our products from SCC 1 we performed an amidation reaction to see how the position and nature of the carboxylic acid affected amidation. All experiments were conducted with 1 mmol of the starting material to ensure consistency of the reaction and consequently the other parameters were constant.

Position and nature of COOH	Total mass recovered (mg)
COOHMe	60.5
COOH	32.1
COOH	8x10-5

Table 4. Data collected from amidation.

Following the amidation reactions it was determined that only the COOHMe and product of COOH at position 4 (product 2b) resulted in a successful reaction. However, it must be noted that product 2b failed to show a NH stretch in the IR. Contrastingly upon analysis of the ^{1}HNMR a singlet at 4.51 was detected corresponding to the 2 hydrogens adjacent to the NH group which could indicate product formation. Although aromatic peaks were present in the ^{1}HNMR further analysis was not viable and thus the correct product cannot be conclusively confirmed due to lack of information and further analysis could not be carried out with minimal yield. The COOHMe product had a present NH stretch in the IR and upon ^{13}CNMR evaluation the formation of 2-(4'-acetyl-[1,1'-biphenyl]-4-yl)-N-benzylacetamide was confirmed. The ortho position proved to be unsuccessful in all regards, although, this was expected due to the significant steric hinderance, and the original starting material purity not being confirmed.

the lack of success in these reactions can be attributed to the experimental procedure. This lack of abundance of appropriate starting material most likely impacted the yield of product 2b due to the impurities present in the starting material. During the experimental procedure of COOH in position 2, ortho, > 1 mmol of the starting carboxylic acid was used due to insufficient yield from SCC 1 which thus impacted the yield of amidation reaction.

In future experiments, improved selectivity and yield may be elucidated through simply increasing the reaction temperature however such conditions can often be energy intensive and unsafe and alternative approaches may be considered. In a separate experiment Liana Allen et al. reported on such methods employing a non-polar solvent, in particular toluene which saw 20 hours to proceed for full conversion into the amide.[19] However this is the uncatalysed and further studies were carried out to increase the reaction rate using a catalyst. Their findings indicated that $ZrCl_4$ saw the best result with 83% conversion in 4 hours.

Experimental

Synthesis of 2-biphenyl benzoic acid **(1a)**

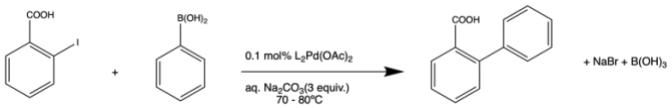

2 – iodobenzoic acid (1.91 g, 7.50 mmol) and phenylboronic acid (1.10 g, 9.00 mmol) was added to round bottomed flask followed by sodium carbonate solution (1.00 M, 22.5 ml). Solution allowed to reach 75 ºC followed by the addition of palladium acetate pre catalyst stock (0.1% mmol, 30.0 ml) to give a pale-yellow solution. After 2 hours 30 minutes the solution remained pale yellow, and no product formation was observed. Another 30.0 ml of catalyst was added and left to heat for an additional hour and left to cool to room temperature, then acidified with aqueous HCl (2M) until pH 2 was achieved. Following filtration, no product was observed and thus the reaction mixture was allowed to proceed undisturbed overnight. Following day product was observed to crash out and following recrystallisation using isopropanol a silver powder of product was

collected (0.90 g: 48.39%) was collected. **M.P.** (161 - 168ºC); **IR** (ATR) ν_{max}/cm^{-1} 2874, 1675; **^{1}H-NMR** (400 MHz, DMSO-d6) δ (ppm) 7.98 (1 H, d, J 7.6), 7.71 (1 H, dd, J 7.7, 1.6), 7.47 (1 H, t, J 7.2), 7.22 (1 H, td, J 7.7, 1.6); **^{13}C-NMR** (101 MHz, DMSO-d6) δ (ppm) 168.19, 140.55, 136.95, 132.49, 130.10, 128.21, 94.13.

Synthesis of 4-(4-acetylphenyl) benzoic Acid (**1b)**

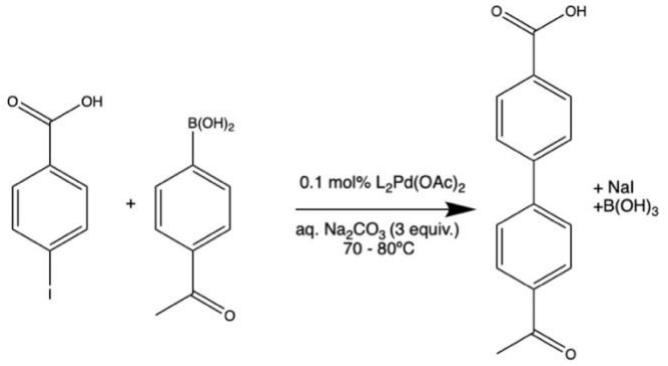

4– iodobenzoic acid (1.86 g, 7.50 mmol) and 4-Acetylphenylboronic acid (1.26 g, 9.00 mmol) was added to round bottomed flask followed by sodium carbonate solution (1M, 22.5 ml). Solution allowed to reach 75 ºC and then followed by the addition of palladium acetate pre catalyst stock (0.1% mmol, 40.0 ml) to give a pale-yellow solution, after 5 minutes a colour change from pale yellow to yellow was observed and a temperature drop from 75ºC to 50ºC. After 45 minutes the solution was observed to be cloudy white. Solution was further heated for 1 hour 30 minutes and then left to cool to room temperature with a cloudy pink colour being observed, acidification with aqueous HCl (2M) was performed until pH 2 was achieved. Following filtration 3.93 g of the crude, the sample exhibited a coloration that ranged between pink and purple. Crude was collected and recrystalised using isopropanol. Product failed to dissolve in hot isopropanol and a hot filtration was conducted leaving a white powder of inorganic material behind. The solvent was evaporated in vaccuo, and the residue was allowed to stand undisturbed overnight. Following recrystallisation product **1b** was obtained as a white powder(24.19%; (0.45 g was collected. **M.P.** (120-122ºC); **Rf** (98:2 DMSO:Methanol) 0.48; **IR** (ATR) ν_{max}/cm^{-1} 3324, 2965, 1670; **^{1}H-NMR** (400 MHz, DMSO-d6) δ (ppm) 6.78 (2 H, d, J 1.6 **(5)**), 6.76 (2 H, d, J 1.6 **(4)**), 6.58 (2 H, d, J 4.2 **(3)**), 6.56 (2 H, d, J 4.1 **(2)**), 1.33 (3 H, s **(1)**).; **^{13}C-NMR** (101 MHz, DMSO-d6) δ (ppm) 197.53 **(8)**, 167.09 **(7)**, 143.34,143.02, 136.27 **(10)**, 130.49, 130.08, 128.99,127.24, 127.20 **(9)**, 25.50 **(6)**.

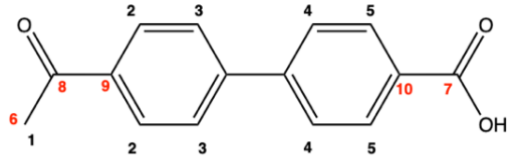

Red = CNMR

Synthesis of ethyl 4'-acetyl-1,1'-biphenyl-4-carboxylate (**2a)**

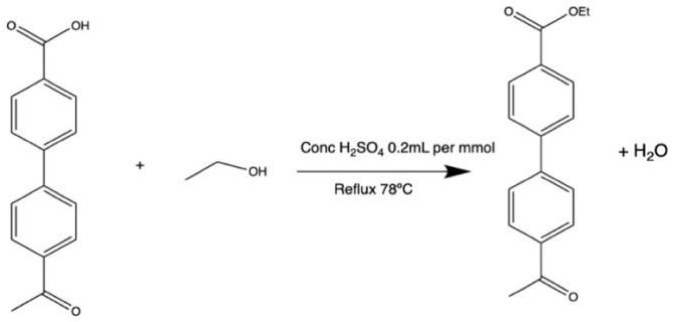

4-(4-acetylphenyl) benzoic Acid (0.45 g, 1.87 mmol) was added to ethanol followed by concentrated sulfuric acid (0.30 mL, 18M) and heated at reflux, a purple solution was observed at 0 minutes and reflux was observed to have begun after 1 hour 20 minutes. Following heating for 4 hours the solution was observed to contain a grey solution and was allowed to cool to room temperature and washed with cold methanol and grey crystals of product **2a** were collected (22.2%; 0.10 g) **M.P.** (104 - 106ºC); **Rf (**98:2 DMSO:Methanol) 0.76; **IR** (ATR) ν_{max}/cm^{-1} 1702; **^{1}H-NMR** (400 MHz, DMSO-d6) δ (ppm) 8.04 (2 H, d, J 2.2, **(3)**), 8.02 (2 H, t, J 1.7**, (4)**), 7.87 –7.84 (2 H, m, **(5)**), 7.84 – 7.82 (2 H, m, **(6)**), 4.32 (2 H, q, J 7.1, **(2)**), 2.60 (3 H, s, **(7)**), 1.32 (3 H, t, J 7.1, **(1)**).; **^{13}C-NMR** (101 MHz, DMSO-d6) δ (ppm) 197.51 **(18)**, 167.07 **(10)**, 143.29 **(14)**,136.32 **(16)**, 130.05 **(12)** 129.84 **(11)**, 128.96 **(15)**, 127.24 **(12)** , 60.87 **(9)**, 26.79 **(19)** , 14.16 **(8).**

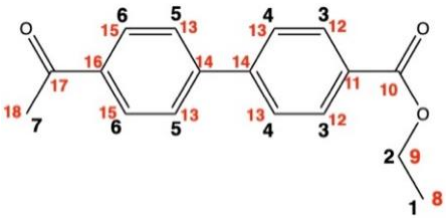

Synthesis of N-benzyl-[1,1'-biphenyl]-4-carboxamide **(2b)**

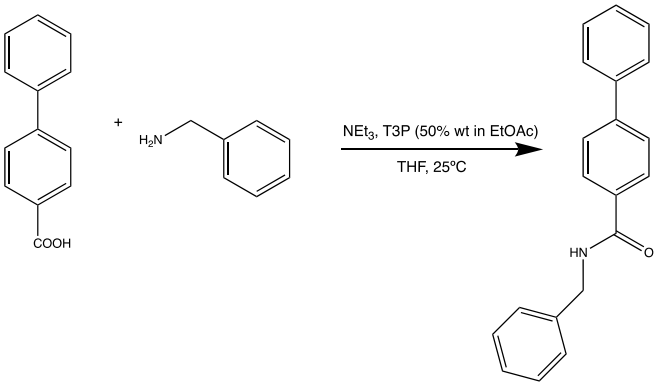

4-biphenylbenzoic acid (0.20 g, 1.00 mmol) was added to THF (5.00 cm^3) followed by triethylamine (0.28 cm^3, 2.00 mmol), benzylamine (0.12 cm^3, 1.10 mmol) and T3P (50wt% in EtOAc, 0.60 cm^3, 2.00 mmol) to form a moderately cloudy mixture. After 1 hour the mixture was observed to be a dark grey solution and after 1 hour 30 the mixture remained to be dark grey. The mixture was stirred until

reaction completion and then diluted with ethyl acetate and washed with HCl (2M, 3.00 x 5.00 ml) followed by NaOH (2M, 2.00 x 5.00 ml) and a layer of emulsion was seen to form. The solution was then washed with further HCl (1M, 2.00 x 5.00 ml) and NaOH (1M 2.00 x 5.00 ml) and the layer of emulsion was seen to dissolve. The solution was then dried over $MgSO_4$ and evaporated in vaccuo; yield was too low to perform a recrystallisation. Yellow crystals of **2b** were collected (6.23 %; 32.1 mg,). **M.P.** (163 - 170ºC); **Rf** (98:2 DMSO:Methanol) 0.95; **IR** (ATR) ν_{max}/cm^{-1} 2247, 1632; **^{1}H-NMR** (400 MHz, DMSO-d6) δ (ppm) 8.01 (1 H, t, J 8.8), 7.84 – 7.69 (2 H, m), 7.55 – 7.45 (1 H, m), 7.42 (1 H, dd, J 7.2, 5.7), 7.34 (1 H, d, J 4.4), 7.25 (1 H, dq, J 8.8, 4.3), 4.51 (2 H, s, J 6.0). Yield collected was too low to perform a **^{13}CNMR.**

Conclusion

We have demonstrated how different parameters affect the reactivity of SCC, both the nature of the boronic acid and aryl halide influence the reaction kinetics and rate. In SCC 1 para - iodine exerted the most significant influence on reaction kinetics due to its lower BDE, resulting in a less endothermic process and a lower activation energy of its transition state according to the Hammond postulate. In SCC 2 EDGs polarised the C - B bond and increased the rate of the transmetallation step. Esterification of SCC 2 products showed the effect of EWG by increasing the reaction rate, highlighting substituent effects. Subsequent amidation on SCC 1 products yielded insufficient data for meaningful analysis likely due to discrepancies in the experimental procedure. The elucidation of these results not only enhances our knowledge and understanding of SCC reactions but also guides future exploration into more efficient and selective design of SCC reactions.

References

(1) The Nobel Prize in Chemistry 2010, https://www.nobelprize.org/prizes/chemistry/2010/summary/, (accessed February 22, 2024).
(2) N. Miyaura and A. Suzuki, Chem. Rev., 1995, **95,** 2457–2483.
(3) S. E. Hooshmand, B. Heidari, R. Sedghi and R. S. Varma, Green Chem., 2019, **21**, 381–405.
(4) S. E. Hooshmand, B. Heidari, R. Sedghi and R. S. Varma, Green Chem., 2019, 21, 381–405.
(5) C. Li, G. Xiao, Q. Zhao, H. Liu, T. Wang and W. Tang, Org. Chem. Front., 2014, **1**, 225–229.
(6) S. V. Sharma, C. Pubill-Ulldemolins, E. Marelli and R. J. M. Goss, Org. Chem. Front., 2021, DOI: 10.1039/d1qo00919b.
(7) Libretexts, Suzuki-Miyaura Coupling, https://chem.libretexts.org/Bookshelves/Inorganic_Chemistry/Supplemental_Modules_and_Websites_(Inorganic_Chemistry)/Catalysis/Catalyst_Examples/Suzuki-Miyaura_Coupling, (accessed March 2, 2024).
(8) I. Hoffmann, B. Blumenröder, S. Onodi neé Thumann, S. Dommer and J. Schatz, Green Chem., 2015, **17**, 3844–3857
(9) T. L. Cottrell, The strengths of chemical bonds, Butterworths, London, 2nd edn, 1958.
(10) G. S. Hammond, J. Am. Chem. Soc., 1955, **77**, 334–338.
(11) J. C. Slater, J. Chem. Phys., 1964, **41**, 3199–3204.
(12) K. Geogheghan, PhD thesis, University of Edinburgh, 2018
(13) P. A. Cox, M. Reid, A. G. Leach, A. D. Campbell, E. J. King and G. C. Lloyd-Jones, J. Am. Chem. Soc., 2017, **139**, 13156–13165.
(14) M. L. Pisarello, B. Dalla Costa, G. Mendow and C. A. Querini, Fuel Process. Technol., 2010, **91**, 1005–1014.
(15) L. A. Wolzak, J. J. Hermans, F. de Vries, K. J. van den Berg, J. N. H. Reek, M. Tromp and T. J. Korstanje, Catal. Sci. & Technol., 2021, **11**, 3326–3332.
(16) A. Alemdar, B. Tan, O. Toksöz, G. Kurtuluş, C. Sesal and Z. Odabaş, J. Mol. Struct., 2023, **1291**, 136100.
(17) D. A. G. Aranda, R. T. P. Santos, N. C. O. Tapanes, A. L. D. Ramos and O. A. C. Antunes, Catal. Lett., 2007, **122**, 20–25.
(18) J. D. St. Denis, C. C. G. Scully, C. F. Lee and A. K. Yudin, Org. Lett., 2014, **16**, 1338–1341.
(19) C. L. Allen, A. R. Chhatwal and J. M. J. Williams, *Chem. Commun.*, 2012, **48**, 666–668.

Appendix

1a) IR + ^{13}CNMR + ^{1}HNMR

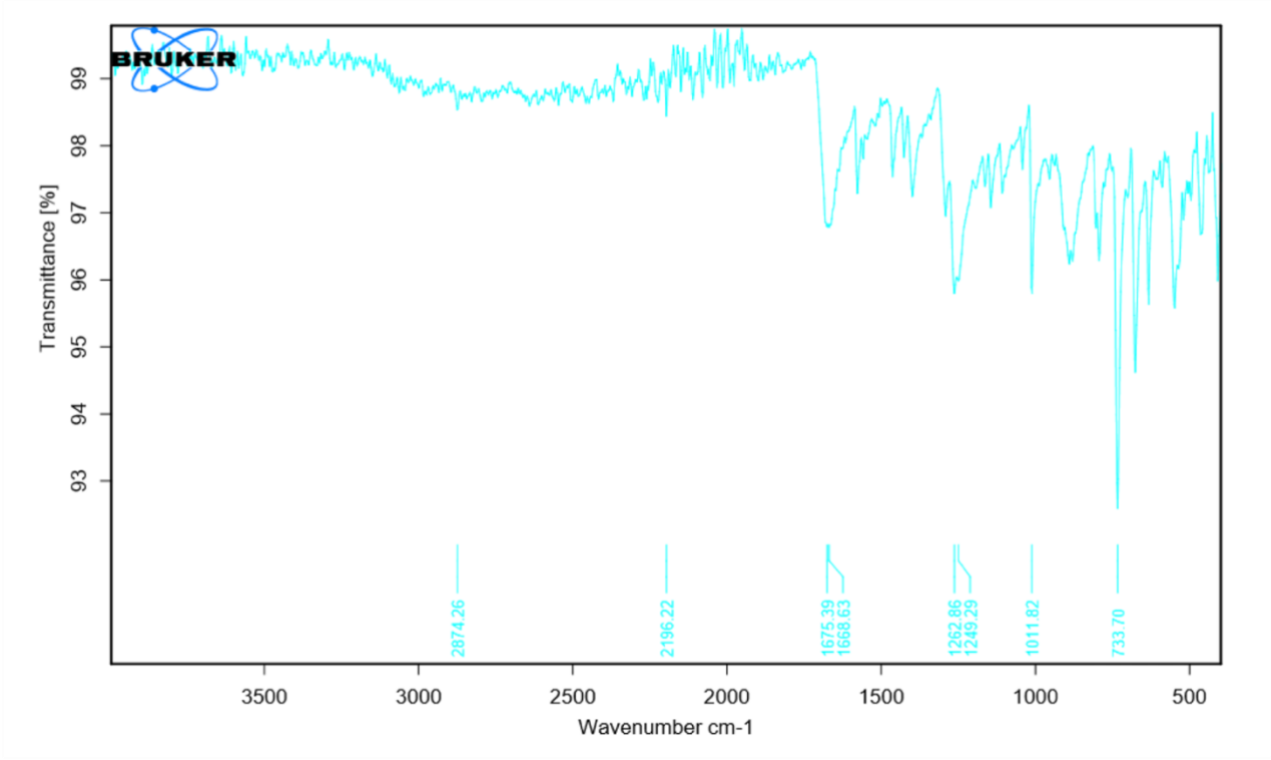

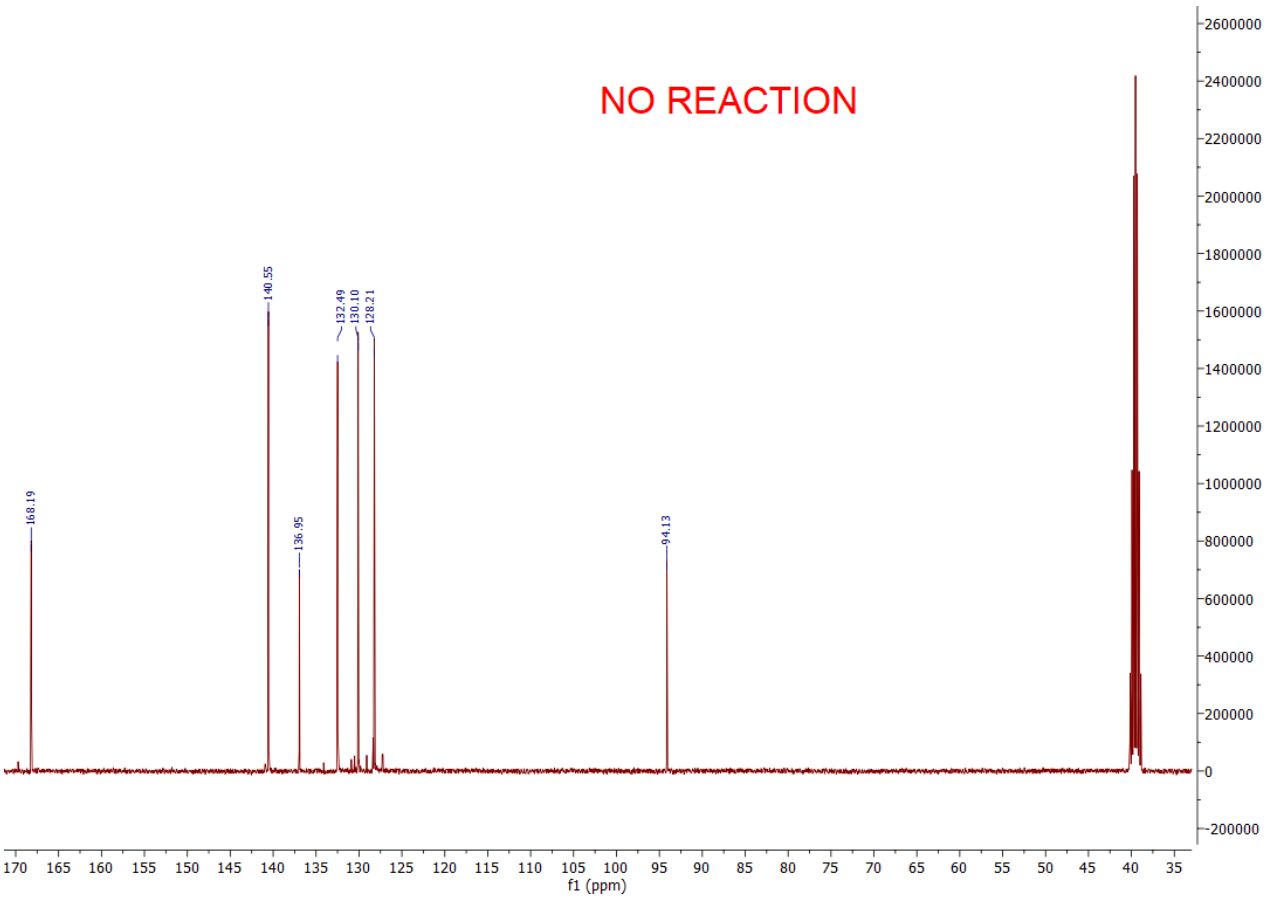

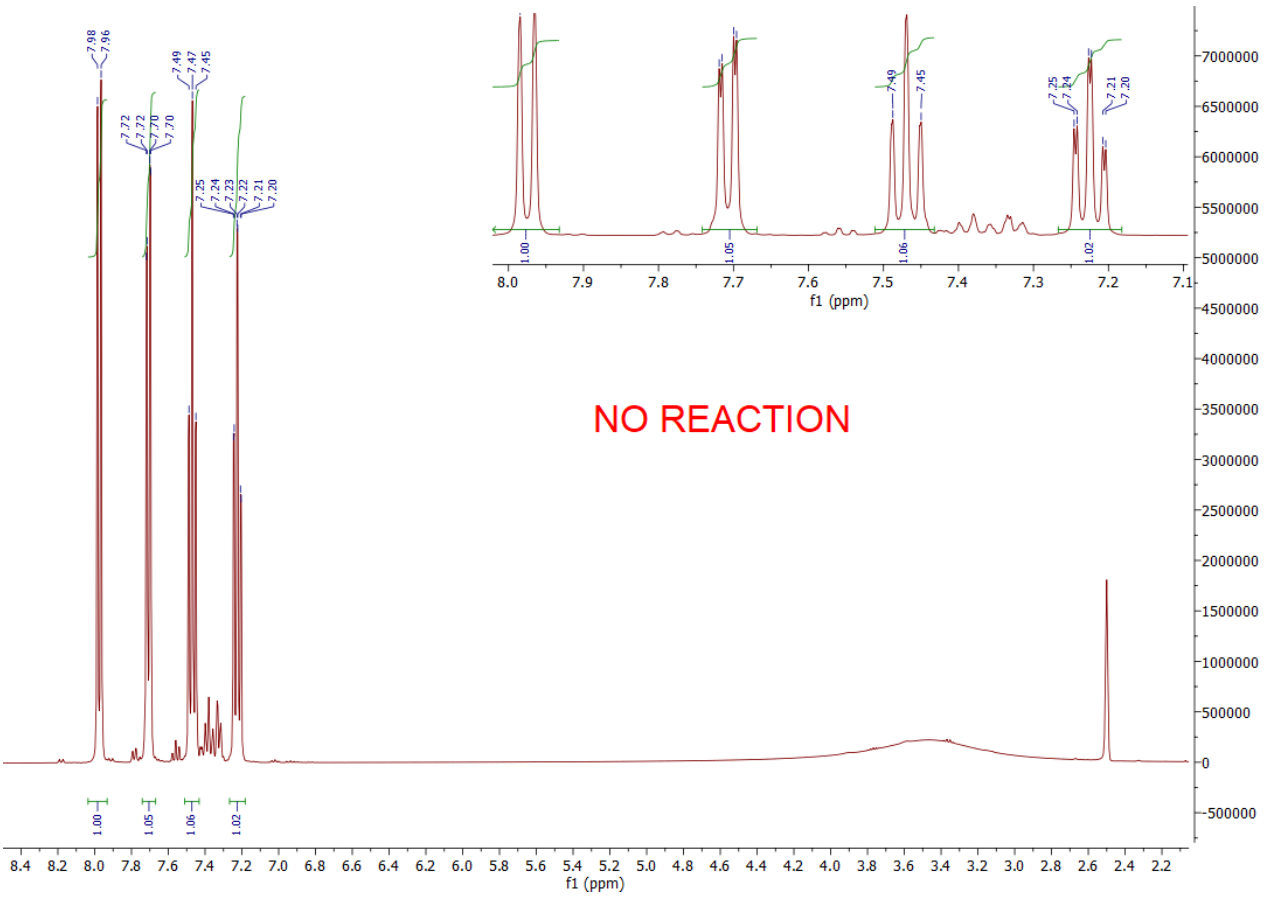

1b) IR + ^{13}CNMR + ^{1}HNMR

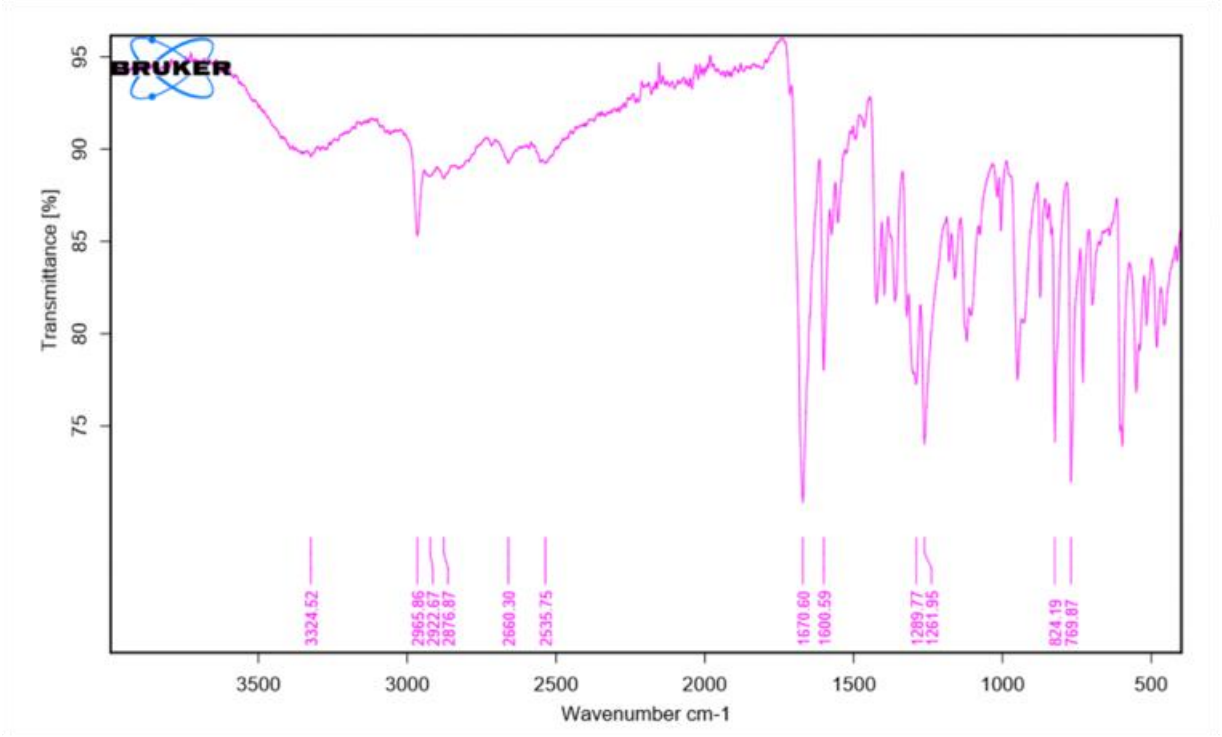

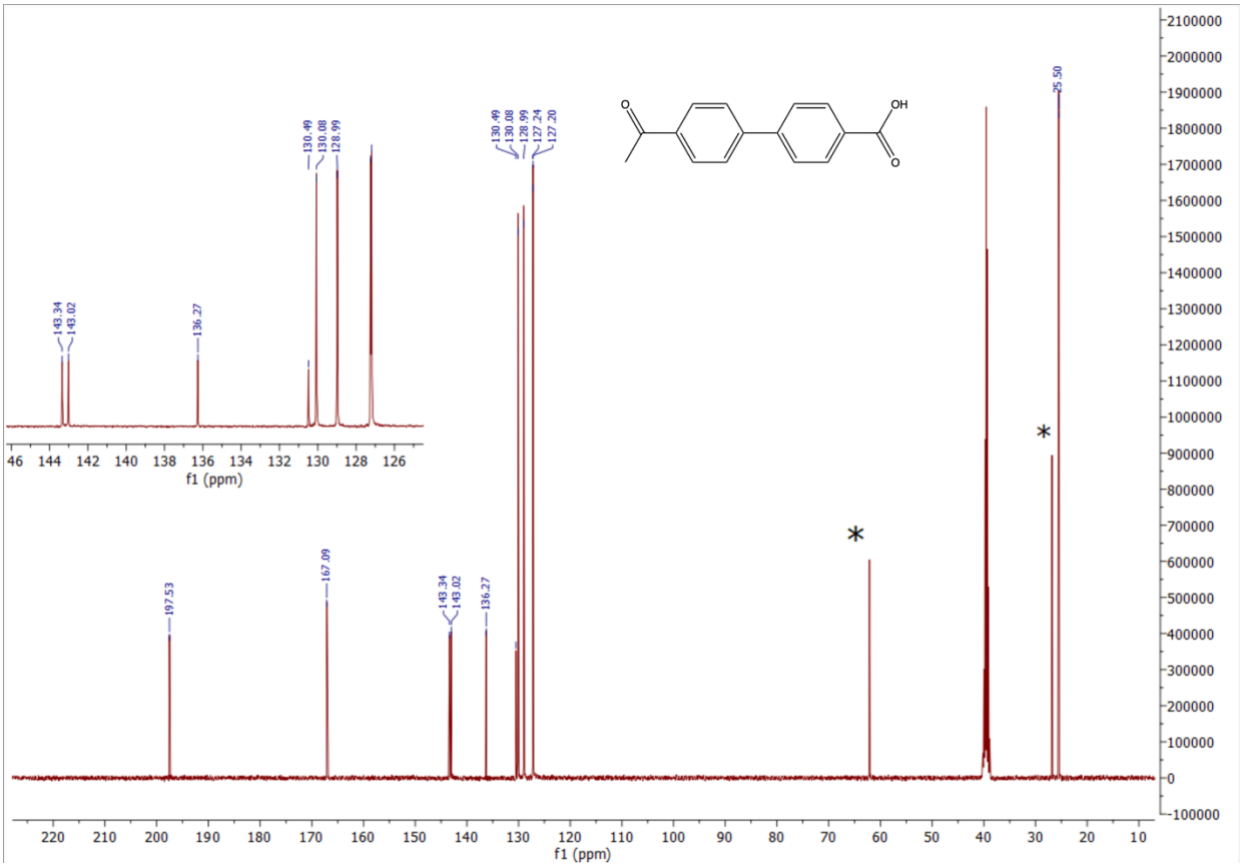
143.34
143.02
136.27
130.49
130.08
128.99
127.24
127.20
125.50
197.53
167.09
OH
O
f1 (ppm)

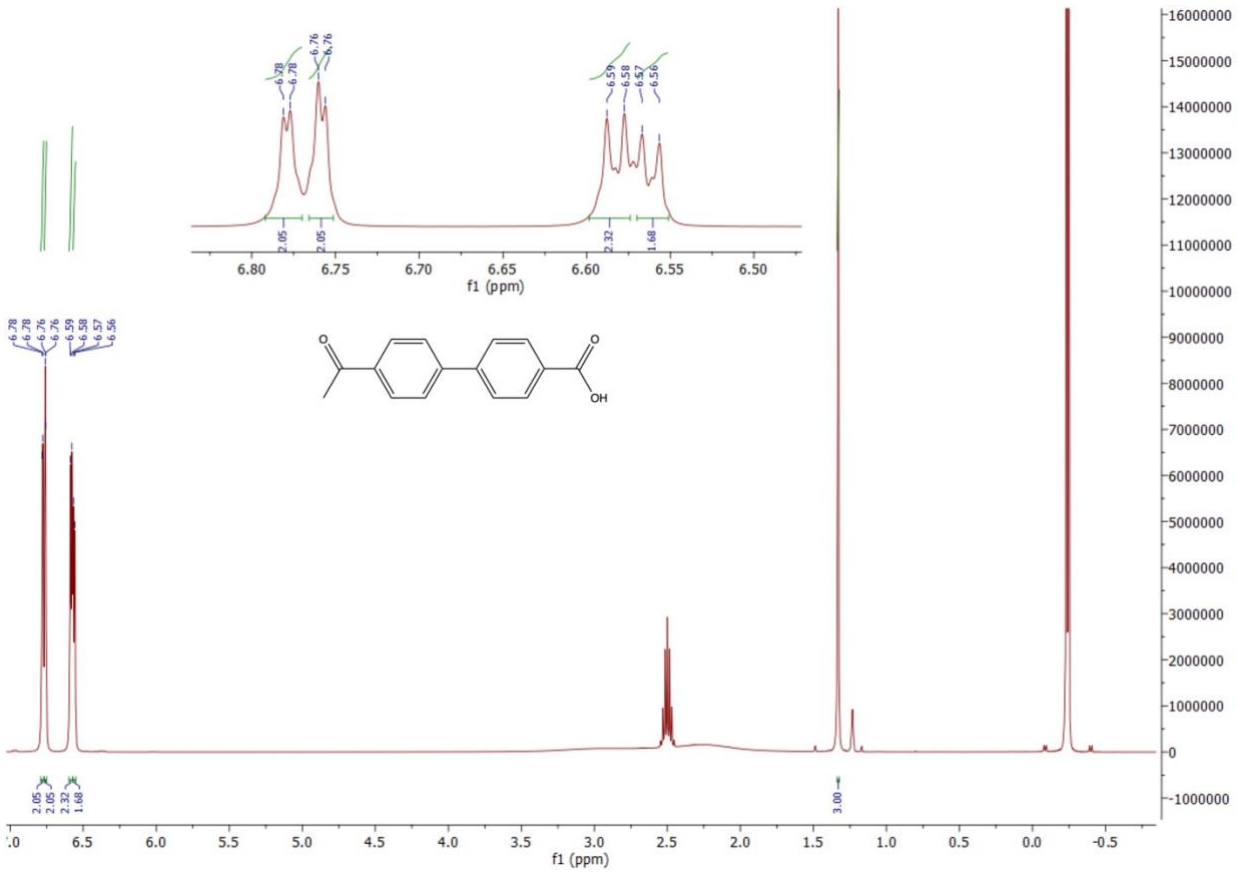
6.78
6.76
6.59
6.58
6.57
6.56
2.05
2.05
2.32
1.68
3.00
OH
O
f1 (ppm)

2a) IR + ^{13}CNMR + ^{1}HNMR

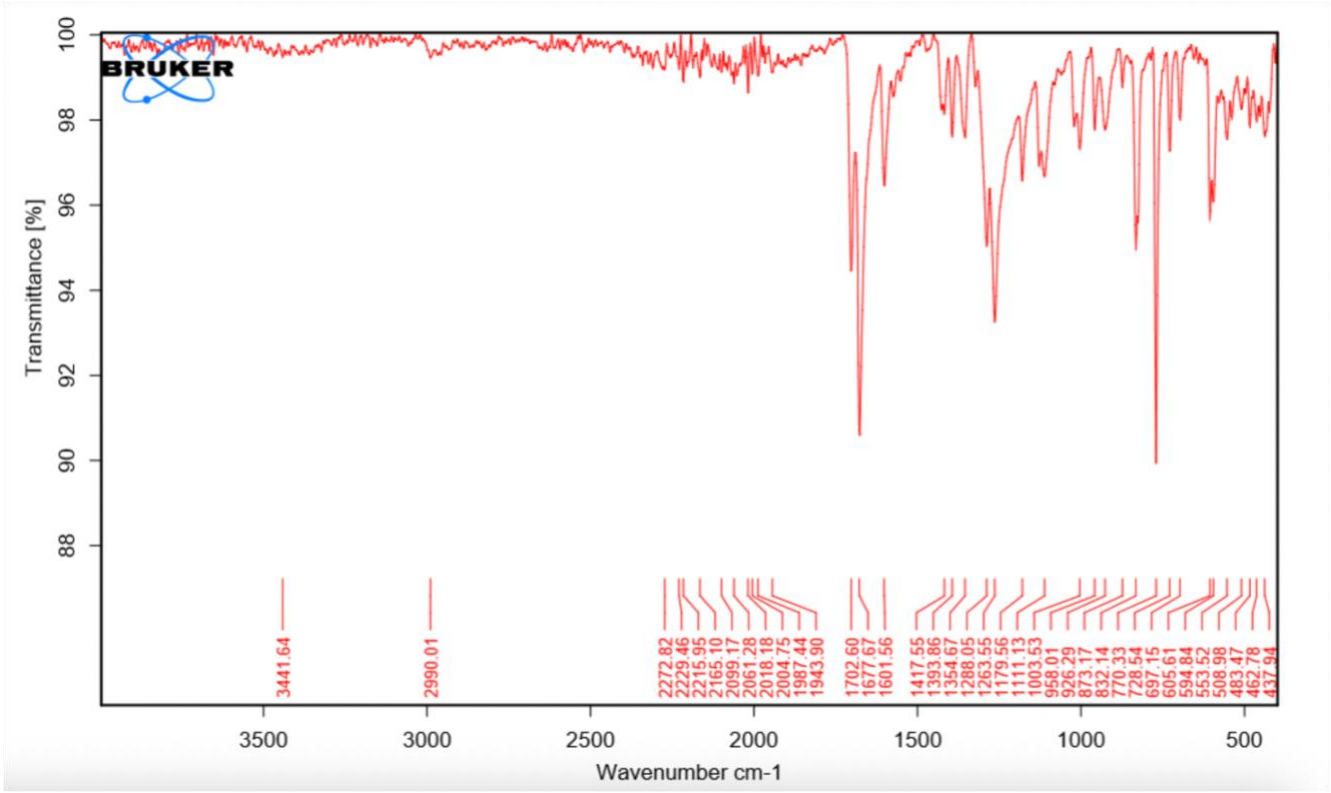

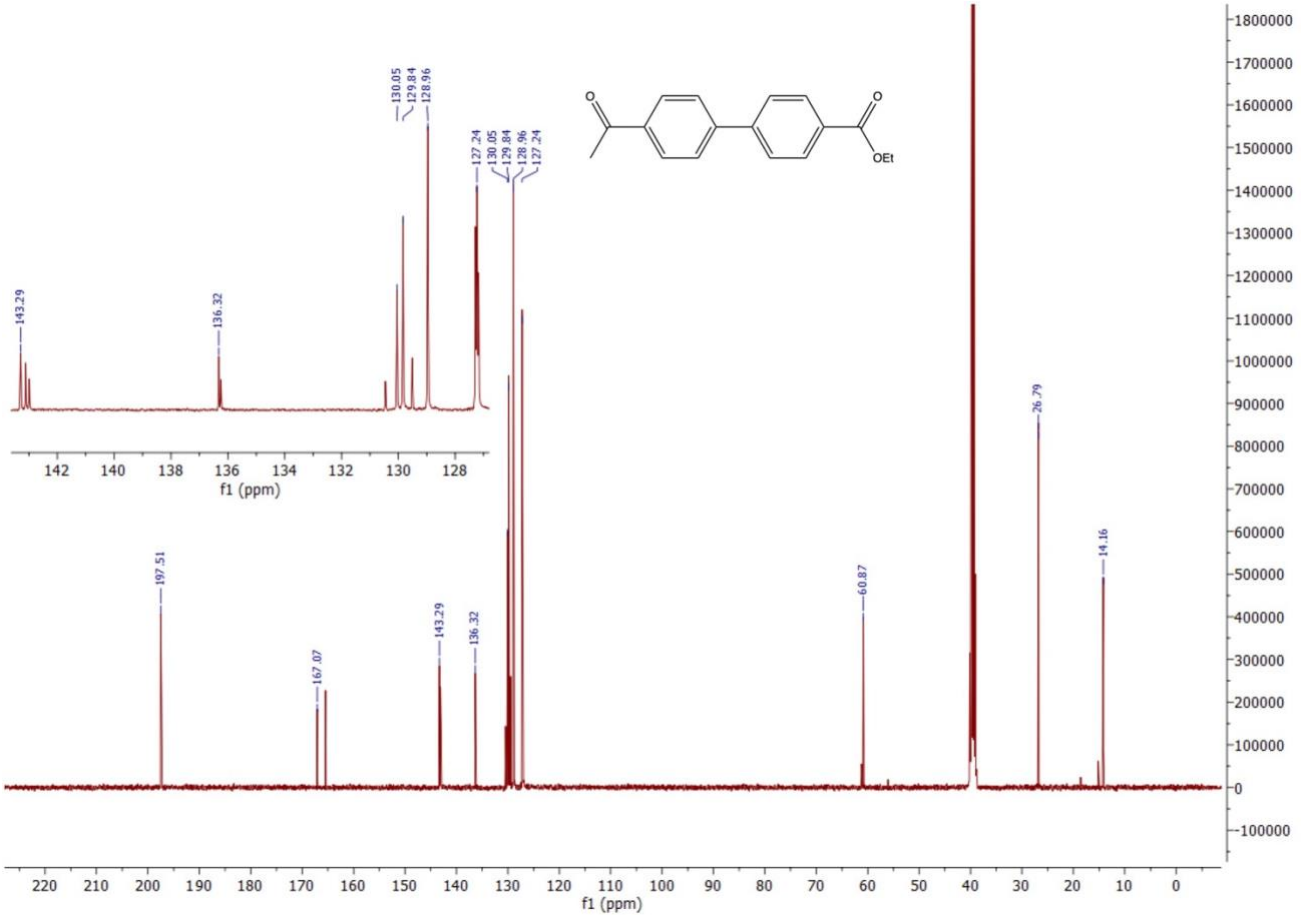

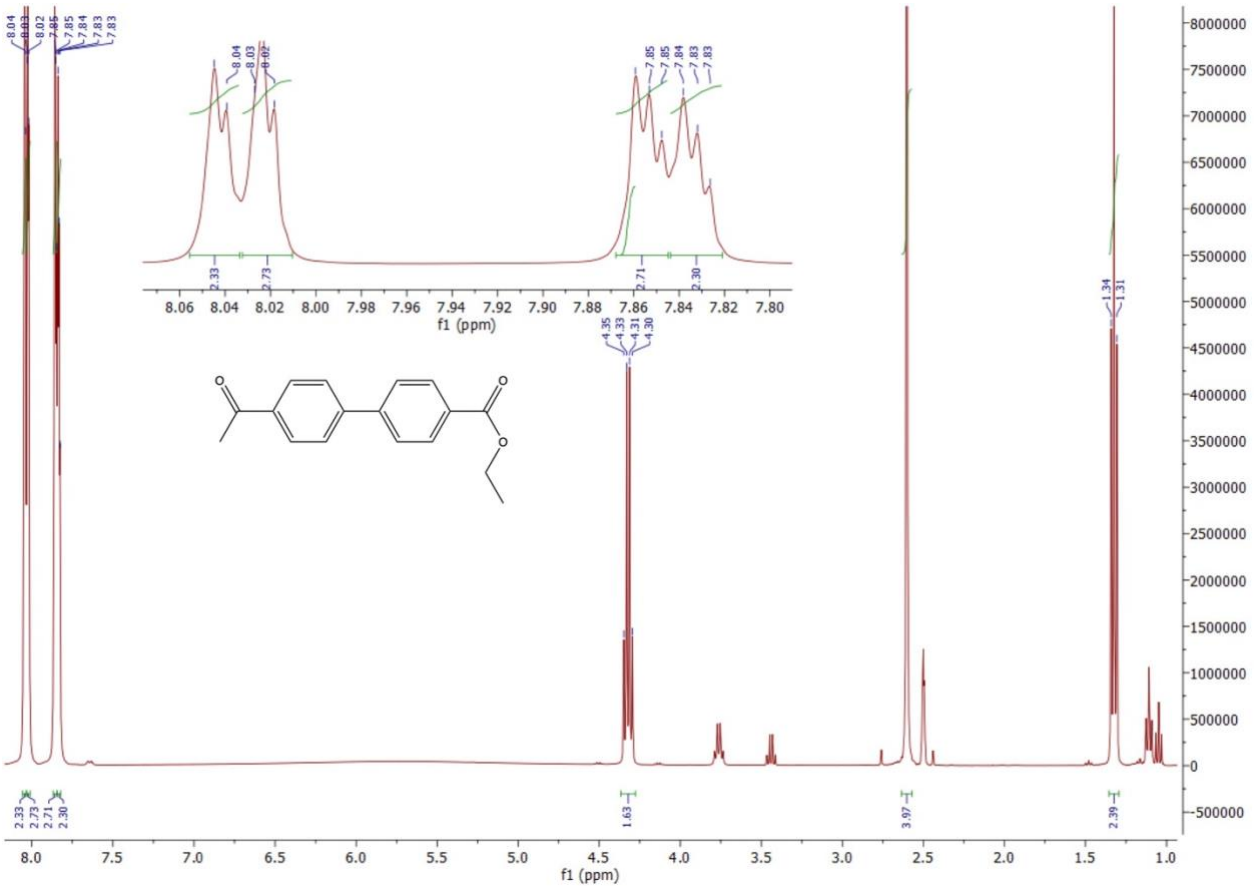
f1 (ppm)
8.04
8.03
8.02
7.85
7.84
7.83
4.35
4.33
4.31
4.30
1.34
1.31
2.33
2.73
2.71
2.30
1.63
3.97
2.39

2b) IR + ^{1}HNMR

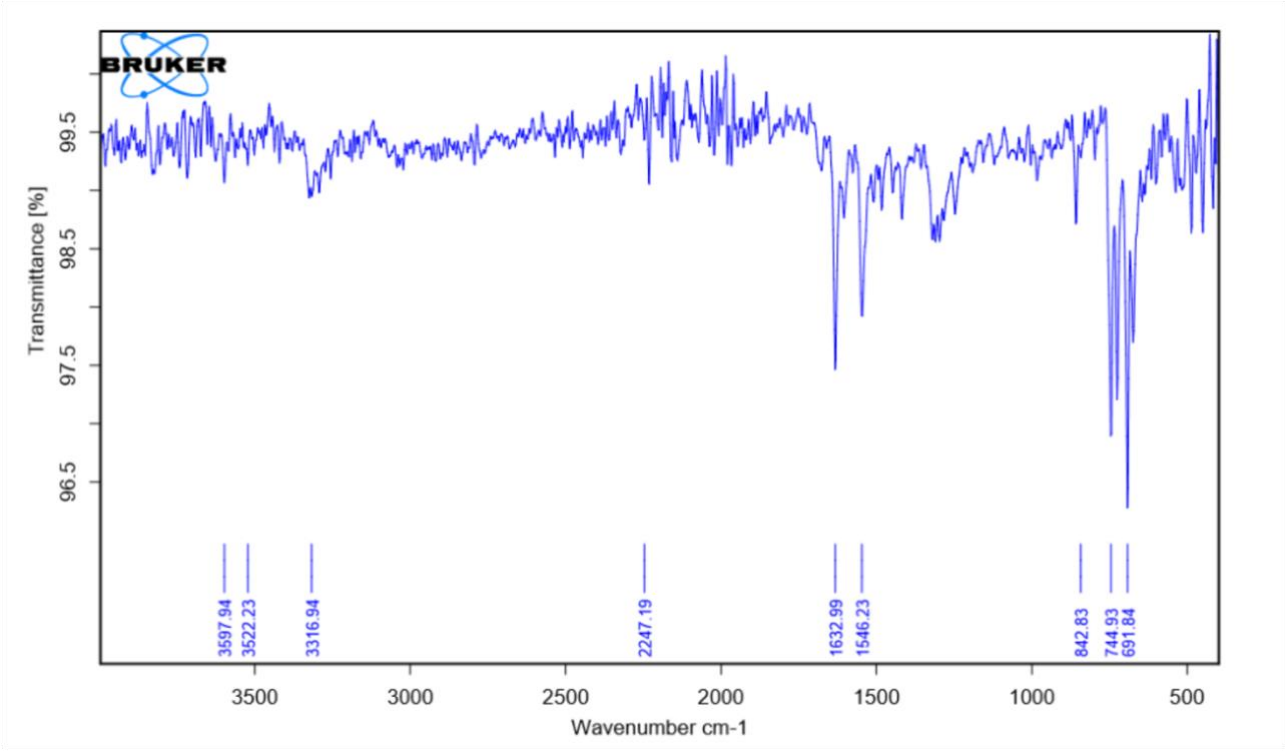
BRUKER
Transmittance [%]
99.5
98.5
97.5
96.5
3597.94
3522.23
3316.94
2247.19
1632.99
1546.23
842.83
744.93
691.84
3500
3000
2500
2000
1500
1000
500
Wavenumber cm-1

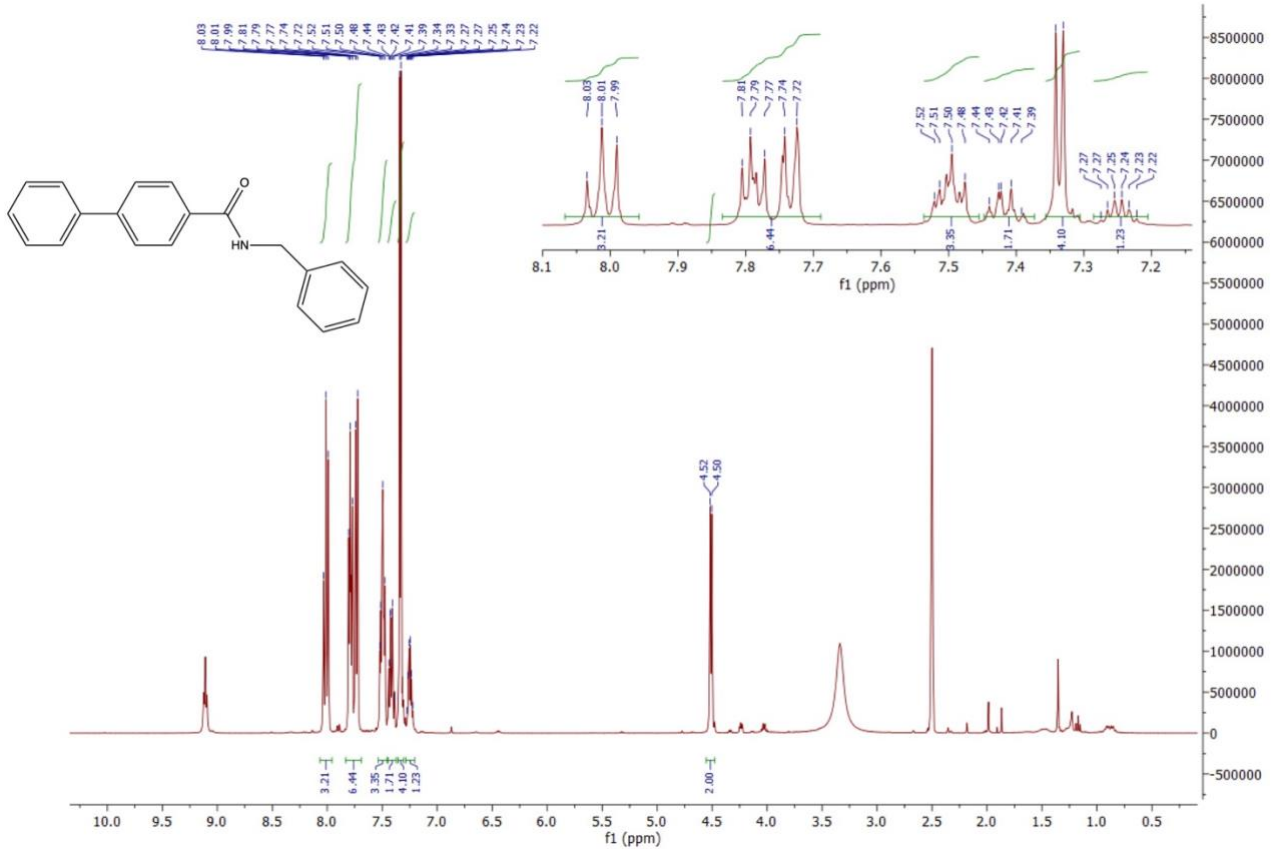
O
HN
f1 (ppm)